

## Design of new biomedical titanium alloy based on d-electron alloy design theory and JMatPro software

Shi-juan DAI, Yu WANG, Feng CHEN, Xin-quan YU, You-fa ZHANG

Jiangsu Key Laboratory of Advanced Metallic Materials, Southeast University, Nanjing 211189, China

Received 3 September 2012; accepted 4 May 2013

**Abstract:** A new kind of  $\beta$  biomedical titanium alloy, Ti–35Nb–4Sn–6Mo–9Zr, composed of non-toxic elements Nb, Mo, Zr and Sn with lower elastic modulus and higher strength was designed based on d-electron alloy design theory and JMatPro software using orthogonal experiment. The microstructure and basic mechanical properties of designed alloy were investigated. The results show that the alloy is composed of single  $\beta$  equiaxed grains after solution treatment at 800 °C. Compared with Ti–6Al–4V, the mechanical properties of the designed alloy are more excellent:  $E=65$  GPa,  $\sigma_b=834$  MPa,  $\sigma_{0.2}=802$  MPa, and  $\delta=11\%$ , which is expected to become a promising new type implanted material. The research approach adopted can reduce the experimental time and cost effectively, and get the ideal experimental results.

**Key words:** titanium alloy; d-electron alloy design theory; JMatPro software; elastic modulus; strength

### 1 Introduction

As a biomedical metal material used for load-carrying implant, titanium alloy has got extensive applications because of its good biocompatibility, mechanical properties and corrosion resistance in the body fluid environment. Recently,  $\beta$  titanium alloy becomes one of the hottest topics in the field of biomedical titanium alloys for its lower elastic modulus compared with  $\alpha+\beta$  titanium alloys [1–3].

For a multi-component titanium alloy, it is difficult to define the relationship of properties–microstructures–ingredients [4,5] because it often involves the complicated interactions between the elements and the microstructures. The design methods on biomedical titanium alloys mainly include d-electron alloy design theory and those based on vague logic and neural network technology at present [6–9]. Reports [6,7] show that Ti–29Nb–13Ta–4.6Zr alloy with low elastic modulus was designed successfully using d-electron alloy design theory. The elastic modulus of the alloy is lower (63 GPa); however, its strength is lower too ( $\sigma_b=590$  MPa,  $\sigma_{0.2}=520$  MPa) compared with Ti–6Al–4V ( $\sigma_b=895$  MPa,  $\sigma_{0.2}=825$  MPa) which is widely used on clinic at present. So far, there is no such

theory which can design a kind of biomedical titanium alloy having lower elastic modulus and higher strength at the same time. JMatPro software developed by the British Thermotech company is a kind of simulation software which can calculate the strength of metal materials. The strength simulation on titanium alloys using JMatPro software is now focused on Ti–Al system and satisfactory results are achieved [10,11]. Based on the d-electron alloy design theory and JMatPro software, a biomedical titanium alloy Ti–35Nb–4Sn–6Mo–9Zr with lower elastic modulus and higher strength is designed, and its mechanical properties are verified.

### 2 Design of alloy

#### 2.1 Choice of alloying elements

The designed alloys are composed of Ti–35Nb (mass fraction, %) matrix and the elements Sn, Zr and Mo. There are two reasons for choosing Sn, Mo and Zr as the alloying elements: one is that these elements have no cytotoxicity and have good biological compatibility with human body [12–14]; the other is that they can act as  $\beta$  stabilizers for forming metastable or near  $\beta$  titanium alloy and have the solid solution strengthening effect on the alloy.

## 2.2 Orthogonal experiment

d-electron alloy design theory is now widely used in the design of titanium alloys with a lower elastic modulus. The theory can predict the range of elastic moduli of titanium alloys by employing two electronic parameters, one is  $B_o$  (characterization of covalent bond strength between Ti and alloying elements), and the other is  $M_d$  (characterization of d-orbital energy, relating to radius and electronegativity of elements). ABDELHADY et al [15] calculated the values of  $\overline{B_o}$  and  $\overline{M_d}$  of different alloys and plotted them on the  $\overline{B_o} - \overline{M_d}$  graph. It is found that the elastic moduli of the alloys decreased with increasing the values of  $\overline{B_o}$  and  $\overline{M_d}$  in the region of  $\beta$  titanium alloy. 29 kinds of  $\beta$ -Ti-Nb alloys were prepared in previous work (the alloys were all composed of single  $\beta$  phase after solid solution treatment). The elastic moduli of these alloys were tested, the values of  $\overline{B_o}$  and  $\overline{M_d}$  were calculated for each alloy and the relationship between  $Y = \overline{B_o} + \overline{M_d}$  and elastic modulus was summarized, as shown in Fig. 1. It can be found that a higher  $Y$  value corresponds to a lower elastic modulus, thus the value  $Y$  can be used as an indicator for designing low modulus titanium alloys.

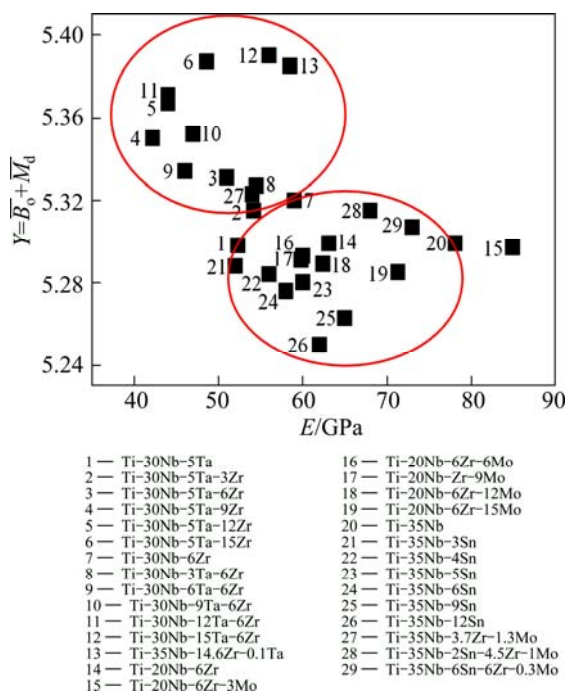


**Fig. 1** Relationship between  $Y = \overline{B_o} + \overline{M_d}$  and elastic moduli of 29 kinds of  $\beta$ -Ti-Nb based alloys previously prepared

Orthogonal test is a mathematical method to carry out multifactor experiments and is widely used in research works for it can analyze the relationship among the factors and the test results with much lower cost and less time [16]. A group of orthogonal tests with three factors, three levels and two indexes were designed in

this work. The two indexes include  $Y = \overline{B_o} + \overline{M_d}$  and the simulated tensile strength  $\sigma_{sm}$  calculated using JMatPro software. The selected factors and levels are shown in Table 1.

**Table 1** Factors and levels of orthogonal experiment

Level	Factor		
	w(Sn)/%	w(Mo)/%	w(Zr)/%
1	3	3	3
2	4	6	6
3	5	9	9

Table 2 lists the orthogonal test program and the results, where tests 1–9 are the orthogonal combinations of the three factors (Sn, Mo and Zr) at different levels (1–3), yielding different values of  $Y$  and  $\sigma_{sm}$ ;  $M_{yi}$  ( $i=1, 2, 3$ ) is the mean value of  $Y$  for a certain factor at level  $i$ , and  $D_y$  is the maximum difference among  $M_{yi}$ . Similarly,  $M_{\sigma i}$  ( $i=1, 2, 3$ ) is the mean value of  $\sigma_{sm}$  for a certain factor at level  $i$ , and  $D_{\sigma}$  is the maximum difference among  $M_{\sigma i}$ .

**Table 2** Orthogonal test program table and results

Test No.	Factor			Index	
	w(Sn)/%	w(Mo)/%	w(Zr)/%	$Y$	$\sigma_{sm}/\text{MPa}$
1	3	3	3	5.3015	421.96
2	3	6	6	5.3163	545.55
3	3	9	9	5.3324	652.49
4	4	3	6	5.3151	500.94
5	4	6	9	5.3308	613.69
6	4	9	3	5.2915	568.98
7	5	3	9	5.3293	572.86
8	5	6	3	5.2905	524.88
9	5	9	6	5.3054	635.96
$M_{y1}$	5.317	5.315	5.295	—	—
$M_{y2}$	5.312	5.313	5.312	—	—
$M_{y3}$	5.308	5.310	5.331	—	—
$D_y$	0.009	0.005	0.036	—	—
$M_{\sigma 1}$	540.000	498.587	505.273	—	—
$M_{\sigma 2}$	561.203	561.373	560.817	—	—
$M_{\sigma 3}$	577.900	619.143	613.013	—	—
$D_{\sigma}$	37.900	120.556	107.740	—	—

$\sigma_{sm}$  is obtained using JMatPro software supposing that the grain size is 15  $\mu\text{m}$ .

### 2.2.1 Effect of alloying elements on $Y$

Considering the value of  $D_y$  of each factor, it is obvious that the most effective factor affecting  $Y$  value is Zr element, and then the Sn element, the least effective factor is Mo element. The effect curves of  $Y$  index are

shown in Fig. 2. It is seen that  $Y$  value increases with increasing Zr content or decreasing Sn or Mo content. If the maximum of  $Y$  value is acquired (the elastic modulus is expected to be the lowest), the alloy composition should be taken as Ti–35Nb–3Sn–3Mo–9Zr.

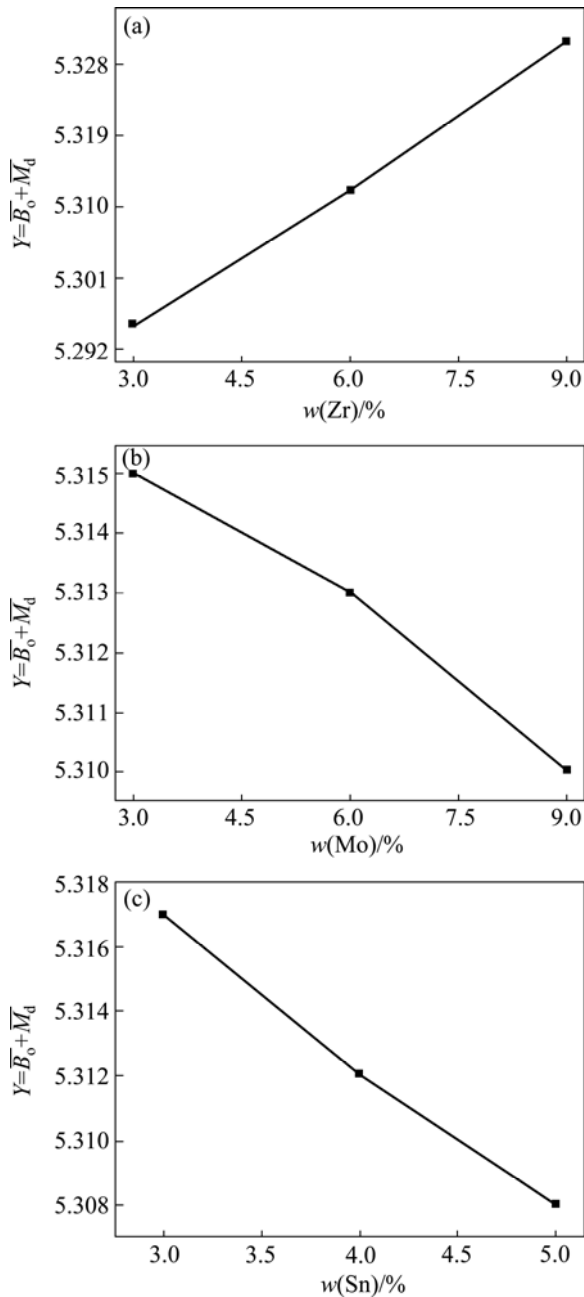


**Fig. 2** Effect curves of  $Y$  index

### 2.2.2 Effect of alloying elements on $\sigma_{sm}$

Considering the values of  $D_\sigma$  of each factor, it is obvious that the most effective factor affecting  $\sigma_{sm}$  is Mo element, and then the Zr element, the least effective factor is Sn element. The effect curve of  $\sigma_{sm}$  index is shown in Fig. 3. It is seen that  $\sigma_{sm}$  value increases with increasing Sn, Mo and Zr content. If the maximum of  $\sigma_{sm}$  value is acquired, the alloy composition should be taken as Ti–35Nb–5Sn–9Mo–9Zr.

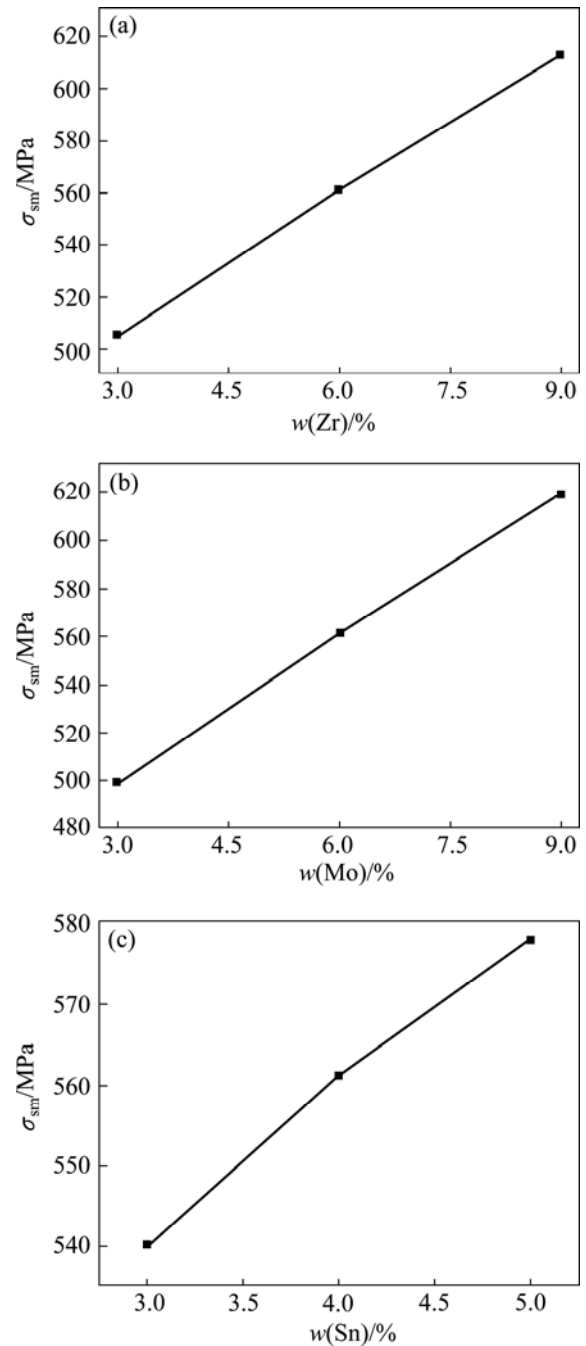


**Fig. 3** Effect curves of  $\sigma_{sm}$  index

### 2.2.3 Determination of alloy composition

It is known that the alloy containing 3% Sn, 3% Mo and 9% Zr has the highest  $Y$  value, while the alloy containing 5% Sn, 9% Mo and 9% Zr has the highest  $\sigma_{sm}$  value. In order to make the alloy achieve lower elastic modulus and higher strength at the same time, the intermediate values of Sn and Mo content in Table 1 (e.g. 4% Sn and 6% Mo) could be adopted, while the Zr content should exceed 9%, because the values of  $Y$  and  $\sigma_{sm}$  increase with Zr content.

LI et al [17] reported that Zr content in the titanium

alloy should not exceed 15% because excess addition of Zr element will cause the weakness of solid solution strengthening effect. Within the above-mentioned 29 kinds of  $\beta$ -Ti–Nb based alloys in Fig. 1, there are 6 kinds of Ti–30Nb–5Ta– $x$ Zr ( $x=0, 3, 6, 9, 12, 15$ )  $\beta$ -titanium alloys. It is found that the elastic moduli of the alloys decrease when the Zr content increases from 3% to 9% and the moduli increases when the Zr content increases from 9% to 15%, as shown in Fig. 4. Therefore, the maximum Zr content of 9% is adopted for ensuring lower elastic modulus of the alloy. It is thus predicted that an alloy having lower elastic modulus and higher strength will be obtained when its composition is taken as Ti–35Nb–4Sn–6Mo–9Zr.

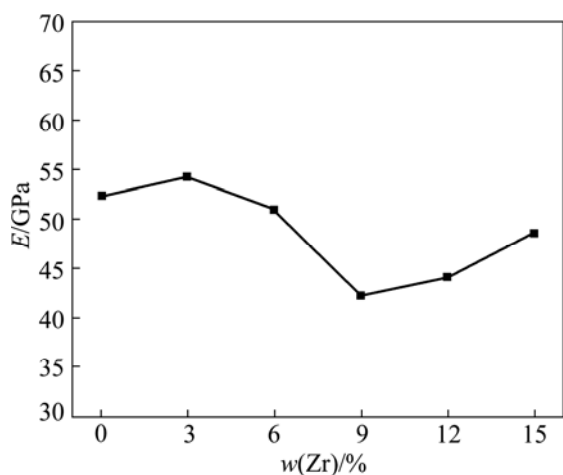


Fig. 4 Relationship between Zr content and elastic modulus of Ti–30Nb–5Ta– $x$ Zr ( $x=0, 3, 6, 9, 12, 15$ )

### 3 Experimental verification of mechanical properties of alloy

#### 3.1 Experimental procedures

The alloys of Ti–35Nb–4Sn–6Mo–9Zr, Ti–35Nb–5Sn–6Mo–3Zr, Ti–35Nb–3Sn–9Mo–9Zr, Ti–35Nb–4Sn–3Mo–6Zr and Ti–35Nb–5Sn–3Mo–3Zr were chosen. Among the above alloys, Ti–35Nb–4Sn–6Mo–9Zr alloy is the designed alloy having higher strength and lower elastic modulus as described above; the other four alloys were selected randomly within the compositional range listed in Table 1 for comparison with Ti–35Nb–4Sn–6Mo–9Zr alloy. The alloys were prepared by arc-melting method in a vacuum melting furnace under an Ar atmosphere. The ingots were re-melted five times for ensuring homogeneity. Then they were hot forged to the plates with a thickness of 3 mm. The hot-forged plates were finally solid solution treated at 800 °C for half an hour and quenched into water.

Using an optical microscope (OM) and transmission

electron microscope (TEM) (Tecnai G2, Holland), the microstructure of the specimens with different compositions, which were burnished, mechanically polished and eroded, was observed. Then, the phase structures of the alloys were analyzed by X-ray diffractometer (XRD) (D8 Discover, Bruker-AXS, Germany). The mechanical properties of the alloys such as tensile strength  $\sigma_b$ , yield strength  $\sigma_{0.2}$  and elongation  $\delta$  were obtained by an electronic universal test machine (CMT 5105, MTS, USA). The elastic modulus  $E$  was calculated according to the slope of the linear portion in the stress–strain curves.

### 3.2 Results and discussion

#### 3.2.1 Microstructure of alloys

The prepared 6 kinds of alloys all have equiaxed and single  $\beta$  phase microstructures after solution treatment with a grain size range of 15–20  $\mu\text{m}$ . However, a thermal  $\omega$  phase is sometimes difficult to be detected by XRD, even if it exists actually in metastable  $\beta$ -type titanium alloys. So, the specimen is observed by TEM. The results show that  $\omega$  phase does not exist in the prepared 6 kinds of alloys and the alloys consist of the single  $\beta$  phase. The OM image, XRD profile, TEM image and the selected-area diffraction pattern of the representative alloy are shown in Fig. 5.

#### 3.2.2 Mechanical properties of alloys

Table 3 shows the mechanical properties of the alloys prepared and those of Ti–6Al–4V alloy [18,19] for comparison. It is seen that Ti–35Nb–4Sn–6Mo–9Zr has lower elastic modulus (65 GPa) and higher strength ( $\sigma_b=834$  MPa,  $\sigma_{0.2}=802$  MPa) compared with the other four alloys prepared. It is found that the strength of Ti–35Nb–4Sn–6Mo–9Zr alloy is comparable to that of Ti–6Al–4V, but its elastic modulus is only 60% of the latter. Therefore, Ti–35Nb–4Sn–6Mo–9Zr alloy is more suitable to be used as implants than Ti–6Al–4V alloy.

Table 4 shows  $\sigma_b$ ,  $\sigma_{sm}$ ,  $E$  and  $Y$  of alloy. It is seen that when the simulated tensile strength  $\sigma_{sm}$  is higher, the tested tensile strength  $\sigma_b$  is higher. It can also be seen that there is a tendency that when the elastic modulus of the alloy is lower, its  $Y$  value is higher, which is in accordance with the relationship shown in Fig. 1.

It is found that  $\sigma_{sm}$  is always lower than  $\sigma_b$ . It may be attributed to the fact that the Scheil–Gulliver solidification model used in JMatPro software ignores the solute diffusion in solid phase and it supposes that the solute diffusion in liquid is complete [20]. During the practical solidification, however, the solute atom is inclined to segregate near the grain boundary which will obstruct the migration of grain boundary and the motion of dislocation, making the tested tensile strength higher than the simulated one.

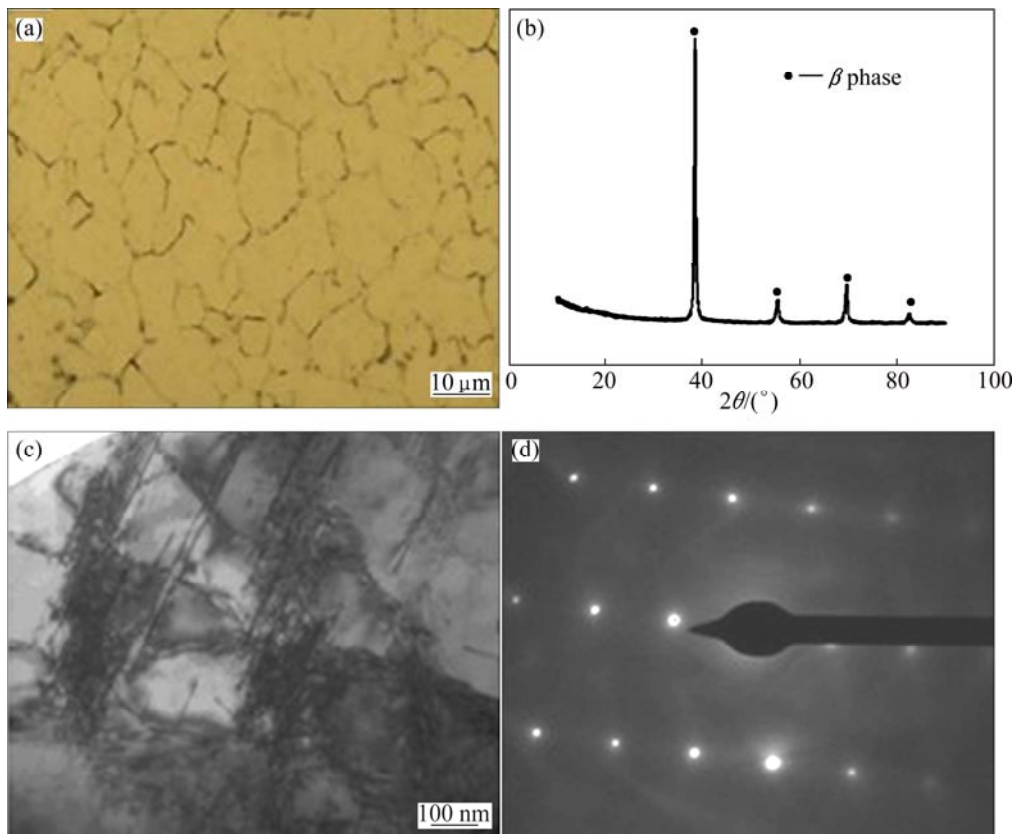


**Fig. 5** Microstructure and XRD diffraction pattern of Ti-35Nb-4Sn-6Mo-9Zr alloy: (a) OM image; (b) XRD profile; (c) TEM image; (d) Selected-area diffraction pattern from (c)

**Table 3** Comparison of mechanical properties between prepared alloys and Ti-6Al-4V alloy [18,19]

Composition	$\sigma_b$ /MPa	$\sigma_{0.2}$ /MPa	$E$ /GPa	$\delta$ /%
Ti-35Nb-4Sn-6Mo-9Zr	834	802	65	11.0
Ti-35Nb-5Sn-3Mo-3Zr	690	668	70	18.0
Ti-35Nb-5Sn-6Mo-3Zr	770	729	85	10.5
Ti-35Nb-3Sn-9Mo-9Zr	833	781	70	10.2
Ti-35Nb-4Sn-3Mo-6Zr	666	654	55	8.9
Ti-6Al-4V	895	825	110	8.0

**Table 4**  $\sigma_b$ ,  $\sigma_s$ ,  $E$  and  $Y$  of alloys

Composition	$\sigma_b$ /MPa	$\sigma_s$ /MPa	$E$ /GPa	$Y$
Ti-35Nb-4Sn-6Mo-9Zr	834	613	65	5.3308
Ti-35Nb-5Sn-3Mo-3Zr	690	460	70	5.2936
Ti-35Nb-5Sn-6Mo-3Zr	770	525	85	5.2905
Ti-35Nb-3Sn-9Mo-9Zr	833	653	70	5.3324
Ti-35Nb-4Sn-3Mo-6Zr	666	501	55	5.3151

## 4 Conclusions

1) Based on d-electron alloy design theory and JMatPro software, a new kind of  $\beta$  biomedical titanium alloy Ti-35Nb-4Sn-6Mo-9Zr with lower elastic

modulus and higher strength is designed using orthogonal experiment.

2) Ti-35Nb-4Sn-6Mo-9Zr alloy displays single  $\beta$  equiaxed grains after solution treatment at 800 °C and the mechanical properties are excellent:  $E=65$  GPa,  $\sigma_b=834$  MPa,  $\sigma_{0.2}=802$  MPa, and  $\delta=11\%$ , which is expected to become a promising new type implanted material.

3) The research approach adopted can reduce the experimental time and cost effectively, and has reference value for designing the biomedical titanium alloys with lower elastic modulus and higher strength.

## References

- [1] WANG L Q, LU W J, QIN J N, ZHANG F, ZHANG D. Influence of cold deformation on martensite transformation and mechanical properties of Ti-Nb-Ta-Zr alloy [J]. Journal of Alloys and Compounds, 2009, 469(1-2): 512-518.
- [2] MATSUMOTO H, WATANABE S, HANADA S. Microstructures and mechanical properties of metastable beta TiNbSn alloys cold rolled and heat treated [J]. Journal of Alloys and Compounds, 2007, 439(1-2): 146-155.
- [3] NIINOMI M, AKAHORI T, KATSURA S, YAMAUCHI K, OGAWA M. Mechanical characteristics and microstructure of drawn wire of Ti-29Nb-13Ta-4.6Zr for biomedical applications [J]. Materials Science and Engineering C, 2007, 27(1): 154-161.

- [4] BIESIEKIERSKI A, WANG J, ABDEL-HADY M, WEN C E. A new look at biomedical Ti-based shape memory alloys [J]. Acta Biomaterialia, 2012, 8(5): 1661–1669.
- [5] DELVAT E, GORDIN D M, GLORANT T, DUVAL J L, NAGEL M D. Microstructure, mechanical properties and cytocompatibility of stable beta Ti–Mo–Ta sintered alloys [J]. Journal of the Mechanical Behavior of Biomedical Materials, 2008, 1(4): 345–351.
- [6] ZHOU Y L, NIINOMI M, AKAHORI T. Changes in mechanical properties of Ti alloys in relation to alloying additions of Ta and Hf [J]. Materials Science and Engineering A, 2008, 483–484: 153–157.
- [7] BRAILOVSKI V, PROKOSHIN S, GAUTHIER M, INAEKYAN K, DUBINSKIY S, PETRZHNIK M. Bulk and porous metastable beta Ti–Nb–Zr(Ta) alloys for biomedical applications [J]. Materials Science and Engineering C, 2011, 31(3): 643–657.
- [8] SUN Y, ZENG W D, HAN Y F. Modeling the correlation between microstructure and the properties of the Ti–6Al–4V alloy based on artificial neural network [J]. Materials Science and Engineering A, 2011, 528(29–30): 8757–8764.
- [9] SAITOVA L R, HOPPEL H W, GOKEN M, SEMENOVA I P, RAAB G I, VALIEV R Z. Fatigue behavior of ultrafine-grained Ti–6Al–4V ‘ELI’ alloy for medical applications [J]. Materials Science and Engineering A, 2009, 503(1–2): 145–147.
- [10] DAISUKE K, NIINOMI M, MORINAGA M. Design and mechanical properties of new  $\beta$  type titanium alloy for implant materials [J]. Materials Science and Engineering A, 1998, 243(1–2): 244–249.
- [11] WEI Q Q, WANG L Q. Influence of oxygen content on microstructure and mechanical properties of Ti–Nb–Ta–Zr alloy [J]. Materials and Design, 2011, 32(5): 2934–2939.
- [12] NIINOMI M. Mechanical biocompatibilities of titanium alloys for biomedical applications [J]. Journal of the Mechanical Behavior of Biomedical Materials, 2008, 1(1): 30–42.
- [13] BERTRAND E, GLORANT T, GORDIN D M, VASILESCU E, DROB P, VASILESEU C, DROB S I. Synthesis and characterisation of a new superelastic Ti–25Ta–25Nb biomedical alloy [J]. Journal of the Mechanical Behavior of Biomedical Materials, 2010, 3(8): 559–564.
- [14] DANIELLE Q M, WISLEI R O, MARIA E P, RUBENS C, AMAURI G. Effects of Zr content on microstructure and corrosion resistance of Ti–30Nb–Zr casting alloys for biomedical applications [J]. Electrochimica Acta, 2008, 53(6): 2809–2817.
- [15] ABDEL-HADY M, HINOSHITA K, MORINAGA M. General approach to phase stability and elastic properties of  $\beta$ -type Ti-alloys using electronic parameters [J]. Scripta Materialia, 2006, 55(5): 477–480.
- [16] BAI W F, ZHANG J H, YAN P, WANG X L. Study on vibration alleviating properties of glass fiber reinforced polymer concrete through orthogonal tests [J]. Materials and Design, 2009, 30(4): 1417–1421.
- [17] LI Q, NIINOMI M, NAKAI M. Effect of Zr on super-elasticity and mechanical properties of Ti–24at%Nb–(0,2,4)at%Zr alloy subjected to aging treatment [J]. Materials Science and Engineering A, 2012, 536: 197–206.
- [18] STOSCHKA M, TAN W, EICHLSEDER W, STOCKINGER M. Introduction to an approach based on the  $\alpha+\beta$  microstructure of elements of alloy Ti–6Al–4V [J]. Procedia Engineering, 2009, 1: 31–34.
- [19] ELIAS L M, SCHNEIDER S G, SCHNEIDER S. Microstructural and mechanical characterization of biomedical Ti–Nb–Zr–(Ta) alloys. Materials Science and Engineering A, 2006, 432(1–2): 108–112.
- [20] BANERJEEA R, NAGB S, FRASERB H L. A novel combinatorial approach to the development of beta titanium alloys for orthopaedic implants [J]. Materials Science and Engineering C, 2005, 25(3): 282–289.

## 基于 d-电子合金设计理论和 JMatPro 软件新型生物医用钛合金的设计

戴世娟, 王煜, 陈锋, 余新泉, 张友法

东南大学 江苏省先进金属材料重点实验室, 南京 211189

**摘要:** 基于 d-电子合金设计理论和 JMatPro 软件, 运用正交试验, 设计了具有较低弹性模量和较高强度且含有无毒元素 Nb、Mo、Zr 和 Sn 的新型生物医用  $\beta$  钛合金 Ti–35Nb–4Sn–6Mo–9Zr, 并对该合金的显微组织和力学性能进行分析。结果表明, Ti–35Nb–4Sn–6Mo–9Zr 合金在 800 °C 下固溶处理后, 由单一的  $\beta$  等轴晶构成。与 Ti–6Al–4V 相比, 该合金具有较优越的力学性能:  $E=65$  GPa,  $\sigma_b=834$  MPa,  $\sigma_{0.2}=802$  MPa,  $\delta=11\%$ , 有望成为新型种植材料。该方法可以有效地降低实验次数, 并得到理想的实验结果。

**关键词:** 钛合金; d-电子合金设计理论; JMatPro 软件; 弹性模量; 强度

(Edited by Xiang-qun LI)